

Characterization of Al₈₅Ni₁₁Y₄ Melt Spun Glass

Matthew D.H. Lay¹, Anita J. Hill¹, Mark A. Gibson² and Timothy J. Bastow¹

¹CSIRO Materials Science and Engineering, Gate 5 Normamby Rd, Clayton South VIC, Australia 3168

²CSIRO Process Science and Engineering, Gate 3 Normamby Rd, Clayton South VIC, Australia 3168

The effect of heat treatment at 300°C on melt-spun Al₈₅Ni₁₁Y₄ ribbons has been studied using nuclear magnetic resonance (NMR) spectroscopy and X-ray diffraction (XRD). XRD spectra show that the melt-spun ribbon is amorphous, after 30 minute heat treatment at 300°C only the amorphous phase and fcc Al are present, but after heat treatment for 75 minutes the Al₃Ni intermetallic phase is also present. ²⁷Al NMR spectra clearly distinguish Al atoms in the amorphous phase from the Al atoms in fcc Al and those from the Al₃Ni intermetallic phase. In addition, the amount in each phase can also be quantified. The complementary information that can be gained from using both NMR and XRD allows us to measure the presence of quenched-in fcc Al precursors in the melt-spun ribbon (detectable only by NMR) and to attribute the NMR-detected intermetallic as the Al₃Ni intermetallic phase (indexed by XRD).

Keywords: *metallic glasses; aluminium alloys; crystallization; nuclear magnetic resonance (NMR)*

1. Introduction

The requirement of a small grain size for strong metals is of paramount importance for alloy design. The connection between yield strength σ_y and grain size d is given by the Hall-Petch relationship [1,2],

$$\sigma_y = \sigma_0 + \frac{k_y}{\sqrt{d}} \quad (1)$$

where σ_0 and k_y are material constants. There are two main strategies for achieving a small grain size: a top down and bottom up approach. The top down approach is to reduce the macroscopic grain size of a conventionally prepared alloy by ball milling or by equal channel angular pressing. Both of these methods produce a smaller grain size accompanied by increasingly heavy deformation as the process continues. The bottom up approach is exemplified by heat treating an amorphous alloy formed by melt spinning (splat cooling) to form nano crystals. This subsequent heat treatment is considered a more controlled process due to its relative simplicity [3].

Nano-structured Al alloys developed by devitrification from melt spun amorphous material are characterized by extremely high strength levels of > 1.2 GPa. For amorphous Al alloys, glass formation is favored for multi-component compositions with aluminium as the major component and transition metals and rare earths as the minor components. The initial devitrification is a primary crystallization of the Al component yielding a microstructure consisting of Al nanocrystals with diameters ranging from 5 nm to 20 nm. A good review on this topic is given by Perepezko and Hebert [4].

Crystallization of glassy alloys is commonly studied with techniques such as XRD and differential scanning calorimetry (DSC). XRD peaks from nanocrystals however can be superimposed on the broad diffraction band from the amorphous matrix in the early stages of evolution which may complicate analysis of XRD spectra. XRD and DSC results have also previously been shown to underestimate the nanocrystalline volume fraction when compared to transmission electron microscopy (TEM) results [5]. Furthermore, previously published isothermal work has been performed for relatively short times that only follow the primary crystallization of fcc Al which occurs prior to crystallization of intermetallic phases [6-8].

In the work reported here the melt spun amorphous alloy $\text{Al}_{85}\text{Ni}_{11}\text{Y}_4$ and the phases developed during heat treatment at 300°C are studied using NMR [9] and XRD. ^{27}Al NMR is used to provide a direct measure of the fraction of each Al-containing phase formed during the devitrification process. This quantification is achieved by line shape simulation of spectra followed by integration of the component line shapes to provide the fraction of Al atoms in the various phases present. These NMR results are compared with XRD results, and the combined use of the two techniques is shown to lead to new insights of the phase evolution during devitrification at 300°C .

2. Materials and Methods

Melt spinning using a substrate velocity of ~ 50 m/s and cooling rate of $\sim 2 \times 10^6$ $^\circ\text{C}/\text{s}$ was used to prepare foil specimens. This resulted in ribbons with a nominal thickness of 50 μm and a width of 1 cm. For NMR and XRD measurements ribbons were cut into pieces with lateral dimensions of ~ 0.5 mm prior to heat treatment. Heat treatments were performed in a muffle furnace under air or a quartz tube furnace under Ar flow.

NMR spectroscopy was performed using naturally abundant ^{27}Al on a Bruker Avance 400 spectrometer. A frequency near 104.2 MHz with a two pulse echo sequence was used to probe static specimens in a 9.4 T magnetic field. To calculate the atomic fraction of each Al-containing phase, the Fourier transformed NMR spectra were peak fitted and integrated with the DMFIT program (ver. 2009) [10].

XRD was performed on the Powder Diffraction beamline at the Australian Synchrotron. Static samples and a X-ray wavelength of 1.001 \AA was used. Peaks were identified using the ICDD-PDF+4 2008 powder diffraction database.

3. Results

NMR spectra of the melt-spun ribbon and samples heat treated for 30 min and 75 min at 300°C are shown in Fig. 1. The sharp peak with a chemical shift of 1635 ppm is due to the fcc Al in the sample while the broader peak centered around 1095 ppm is associated with the Al contained in the remaining amorphous matrix of the sample. The peak at 660 ppm in the sample heat treated at 300°C for 75 minutes is attributed to an Al-containing intermetallic phase. XRD will be used to identify the intermetallic phase. Note that some fcc Al is observed to have been crystallized out in the starting material. These fcc Al crystals may be the sub-nanometer precursor particles proposed by Nitsche et al. [11].

The area under the NMR peaks can be used to quantify the atomic fraction of Al atoms in each phase. Results for the calculated atomic percentages from Fig. 1 are as follows: (i) for the as-quenched melt-spun ribbon (i.e. 0 minutes at 300°C), 2.6 at. % of the Al in the starting material is in the fcc phase and 97.4 at. % of the Al is amorphous; (ii) for the sample heated for 30 minutes, 67 at. % of the Al is in the fcc phase and 23 at. % is amorphous; (iii) for the sample heated for 75 minutes, 73 at. % of the Al is in the fcc phase, 6 at. % is amorphous and 21 at. % is in an intermetallic phase.

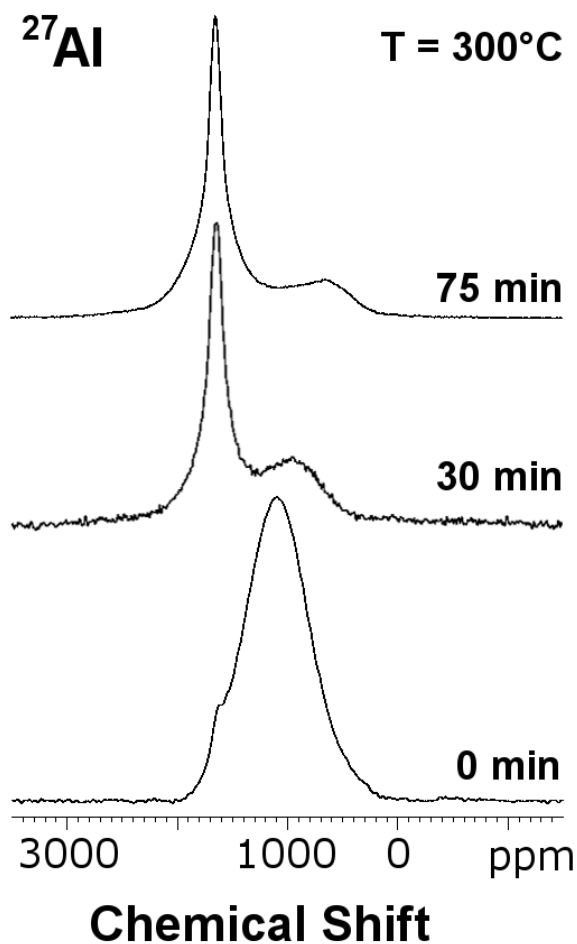


Fig. 1 NMR spectra for heat treated samples at 300°C for 0, 30, and 75 minutes.

The XRD spectrum of the starting material does not contain fcc Al peaks and only broad bands consistent with amorphous structure are present (Fig. 2). This is despite NMR results indicating 2.6 at. % fcc Al. It is possible that the fcc Al is present as nanocrystals at too low a concentration to be resolved or that the crystals are too small to produce diffraction peaks that can be distinguished over the broad amorphous peak. Samples isothermally heat treated for 30 minutes show fcc Al peaks superimposed on the broad amorphous structure peaks, consistent with NMR. Heat treatment for 75 minutes at 300°C leads to XRD peaks corresponding to intermetallic Al₃Ni as well as those for fcc Al. This XRD result after 75 minutes at 300°C allows us to attribute the NMR peak at 660 ppm in Fig. 1 to the Al₃Ni intermetallic. Scherrer analysis of the fcc Al peaks in Fig. 2 gives nanocrystal dimensions of ~25 nm and ~45 nm after heat treatments for 30 minutes and 75 minutes, respectively, at 300°C.

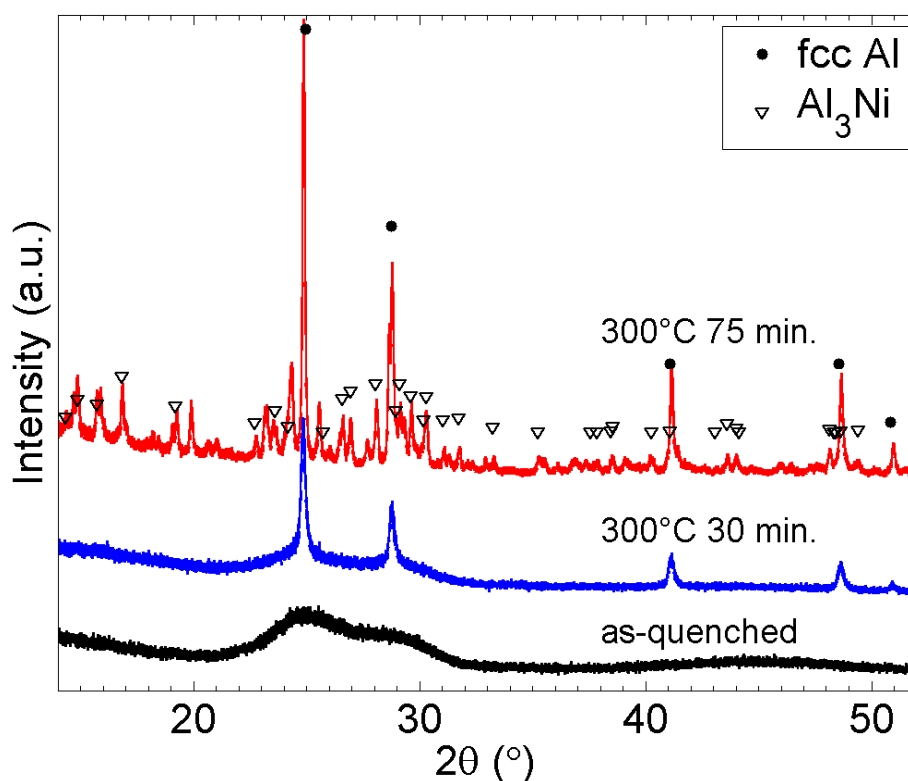


Fig. 2 X-ray diffraction spectra of samples heat treated at 300°C for 0, 30, and 75 minutes.

4. Discussion

It is shown here that NMR detects the presence of the fcc crystals prior to their detection by XRD. The main reason for this is that shifts in the resonance frequency in NMR are sensitive to the local nuclear environment of the Al atoms and do not require long range order. Furthermore, NMR is element specific; only the aluminium atoms are detected. The X-ray scattering in our as-quenched material is dominated by the Ni and Y scattering because the form factors are larger than that for Al. It is also possible the fcc Al precursors crystals in the melt spun ribbon are observed by NMR but not by XRD due to their low volume fraction and small size which may require higher concentrations to be discerned from TEM or XRD [12].

Analysis of NMR spectra gives a clear quantitative picture of the crystallization pathway. These results are important in determining the optimal heat treatment for formation of fcc Al nanocrystals to improve the strength of metallic glasses while avoiding intermetallic formation which may lead to a reduction in hardness [7] or embrittlement [13,14].

5. Conclusion

The technique of solid state NMR using ^{27}Al as a probe provides an appealing method for analyzing quantitatively for the nano-phase Al component in partially crystallized melt spun alloys as well as following the phase transformation pathways during devitrification of amorphous alloys. NMR is shown to be sensitive to the presence of Al nanocrystals at concentrations or sizes below the detection limit of XRD. Further heat treatments at different temperatures will allow for more in-depth analysis and are the subject of future work.

Acknowledgements

Part of this research was undertaken on the Powder Diffraction beamline at the Australian Synchrotron, Victoria, Australia. The authors would like to thank Dr Dario Buso and Dr Paolo Falcaro of CSIRO for performing XRD on the samples and Dr Kate Nairn for helpful discussion. MDHL is funded through the CSIRO Office of the Chief Executive postdoctoral program.

References

- [1] K. J. Kurzydowski: *Scripta Metall. Mater.* 24 (1990) 879-883.
- [2] B. Raeisinia and C. W. Sinclair: *Mater. Sci. Eng. A* 525 (2009) 78-82.
- [3] Y. H. Kim, K. Hiraga, A. Inoue, T. Masumoto, and H. H. Jo: *Mater. Trans. JIM* 35 (1994) 293-302.
- [4] J. H. Perepezko and R. J. Hebert: *JOM* 54 (2002) 34-39.
- [5] T. Gloriant, M. Gich, S. Surinach, M. D. Baro, and A. L. Greer: *Mater. Sci. Forum* 343-346 (2000) 365-370.
- [6] Z. H. Huang, J. F. Li, Q. L. Rao, and Y. H. Zhou: *Mater. Sci. Eng. A* 489 (2008) 380-388.
- [7] K. L. Sahoo, M. Wollgarten, J. Haug, and J. Banhart: *Acta Mater.* 53 (2005) 3861-3870.
- [8] K. L. Sahoo, A. K. Panda, S. Das, and V. Rao: *Mater. Lett.* 58 (2004) 316-320.
- [9] C. P. Slichter: *Principles of Magnetic Resonance*, (Springer-Verlag, 1990).
- [10] D. Massiot, F. Fayon, M. Capron, I. King, S. Le Calve, B. Alonso, J. O. Durand, B. Bujoli, Z. H. Gan, and G. Hoatson: *Magn. Reson. Chem.* 40 (2002) 70-76.
- [11] H. Nitsche, F. Sommer, and E. J. Mittemeijer: *J. Non-Cryst. Solids* 351 (2005) 3760-3771.
- [12] H. W. Yang, J. Wen, M. X. Quan, and J. Q. Wang: *J. Non-Cryst. Solids* 355 (2009) 235-238.
- [13] H. S. Kim, P. J. Warren, B. Cantor, and H. R. Lee: *Nanostruct. Mater.* 11 (1999) 241-247.
- [14] Z. C. Zhong, X. Y. Jiang, and A. L. Greer: *Mater. Sci. Eng. A* 226 (1997) 531-535.